SCIENCE CHINA
Earth Sciences

• RESEARCH PAPER •

August 2010 Vol.53 No.8: 1241–1248
doi: 10.1007/s11430-010-3034-z

The lightning activities in super typhoons over the Northwest Pacific

PAN LunXiang[1,2], QIE XiuShu[1*], LIU DongXia[1,2], WANG DongFang[1] & YANG Jing[1]

[1] *LAGEO, Institute of Atmospheric Physics, Chinese Academy of Sciences, Beijing 100029, China;*
[2] *Graduate University of Chinese Academy of Sciences, Beijing 100049, China*

Received January 18, 2009; accepted August 31, 2009; published online June 9, 2010

The spatial and temporal characteristics of lightning activities have been studied in seven super typhoons from 2005 to 2008 over the Northwest Pacific, using data from the World Wide Lightning Location Network (WWLLN). The results indicated that there were three distinct lightning flash regions in mature typhoon, a significant maximum in the eyewall regions (20–80 km from the center), a minimum from 80–200 km, and a strong maximum in the outer rainbands (out of 200 km from the center). The lightning flashes in the outer rainbands were much more than those in the inner rainbands, and less than 1% of flashes occurred within 100 km of the center. Each typhoon produced eyewall lightning outbreak during the periods of its intensification, usually several hours prior to its maximum intensity, indicating that lightning activity might be used as a proxy of intensification of super typhoon. Little lightning occurred near the center after landing of the typhoon.

super typhoon, lightning, WWLLN, the Northwest Pacific

Citation: Pan L X, Qie X S, Liu D X, et al. The lightning activities in super typhoons over the Northwest Pacific. Sci China Earth Sci, 2010, 53: 1241–1248, doi: 10.1007/s11430-010-3034-z

Nearly one-third of the tropical cyclones in the world generate over the Western Pacific, and China is one of the most severely typhoon-affected countries. There are about seven to eight typhoons make landfalls in China every year [1]. Typhoon brings plenty of water vapours and mitigates some of the regional drought. However, heavy rainfall and strong winds accompanying typhoon produced great casualties. Little is known about the frequency and distribution of lightning in typhoon, mainly because typhoons occur over the ocean and far from land-based lightning detection networks. Jorgensen et al. [2] found that vertical motions in oceanic convection and in hurricanes were much weaker than in midlatitude storm systems. Christian et al. [3] analyzed annual global lightning distribution and confirmed that lightning occurs mainly over terrestrial areas, with an average land/ocean ratio of ~10:1. Molinari et al. [4] investigated the spatial and temporal distribution of cloud-to-ground (CG) lightning in hurricane Andrew (1992) by using the NLDN data and divided the hurricane into three regions based on its electrical characteristics, eyewall, inner bands, 40–100 km from the center and near-zero lightning density in this region, and outer rainbands, beginning from 100 km and reaching peak flash density at 190 km from the center. The average flash frequency was 4400 fl day^{-1} within a 300 km region of the hurricane center. Samsury and Orville [5] studied two storms, hurricane Hugo and Jerry. Hugo produced only 33 CG lightning flashes and Jerry 691 in 18 hour, far less than that in Andrew. The ratio of positive CG flashes for both storms was much higher than the average value detected by the network. Lyons and Keen [6] described lightning variations in an unnamed tropical storm, mostly over land, in 1987, and in Hurricanes

*Corresponding author (email: qiex@mail.iap.ac.cn)

Diane (1984), Florence (1988), and briefly in Hurricane Elena (1985). It was found that both Hurricanes Diane and Florence showed significant outbreaks of lightning near the center before or during their intensification. Molinari et al. [7] used NLDN lightning data to examine the hourly lightning evolution in nine Atlantic hurricanes during 1985 to 1991. The results were consistent with that of Hurricane Andrew, and the eyewall flashes were episodic and occurred during or just before the period of intensification. Cecil and Zipper [8] used satellite-based OTD data to analyze dozens of tropical cyclones (TCs). Cecil et al. [9, 10], using TRMM satellite-based LIS data, studied 261 overpasses of 45 TCs. They showed that the lightning radial distribution is similar to Molinari et al. [7], in which lightning density maxim were in eyewall and outer rainband regions, with a lightning density minimum in inner rainband region. Squires and Businger [11] combined the LLDN, TRMM, and WP-3D data to examine two of the strongest hurricanes Rita and Katrina; each hurricane produced eyewall lightning outbreaks during three periods, the most rapid intensification, the eyewall replacement cycles, and encompassed the maximum intensity for each storm. Shao et al. [12] studied lightning in Katrina and Rita based on the data from LASA. Solorzano et al.[1)] studied two Atlantic hurricanes and three western Pacific typhoons with WWLLN data; the results were similar to Molinari et al. [7].

Above mentioned studies showed many promising results of lightning activities in tropical cyclones before they made landfall, utilizing data from satellite-based lightning detectors (e.g., OTD, LIS) or grounded-based regional lightning networks. However, the regional lightning network can only detect lightning near seashore, and the satellite can only detect a few minutes and regions of some storms, and it is hard to figure out the whole picture of lightning characteristics. The WWLLN is a world-wide network, which detects lightning activities globally. The previous WWLLN-based studies mainly focused on the hurricanes over the Atlantic Ocean, and few studies about Western Pacific. Does the lightning in typhoons over the Western Pacific have similar characteristics to Atlantic Ocean's? Where does the lightning tend to be distributed in typhoons? What is the relationship between lightning activity and typhoon intensity? This paper tries to answer these questions.

1 Data and methodology

The lightning data used in this study are from the World Wide Lightning Location Network (WWLLN), which detects lightning activity occurred anywhere in the globe. The WWLLN provides almost real time lightning locations globally by measuring the very low frequency (VLF) radiation (3–30 kHz) emanating from lightning discharges. These VLF signals can be received thousands of kilometers from the source [13]. For a lightning flash to be accurately detected with error analysis, the VLF radiation from a flash must be detected at a minimum of 5 of the network's 40 receivers around the world. Every receiving station consists of a whip antenna to measure VLF electric field, a GPS antenna for accurate timing, preamplifying electronics, and an internet-connected processing computer. Each receiver locally processes a flash's waveform and sends the time of group arrival to the central processing station for location in Washington University.

A number of investigations [14–17] have combined local lightning location observations to estimate the detection efficiency of the WWLLN in some regions. Lay et al. [14] found a very low detection efficiency of 0.3% in Brazil. Rodger et al. [16] compared the WWLLN data in Australia with the local Australia lightning location network, Kattron, and found a ~13% total lightning detection efficiency, ~26% CG detection efficiency, and a ~10%intracloud lightning efficiency in Australia. Jacobson et al. [17] found an efficiency of about 4% of WWLLN for the flash with a peak current I_p greater than 40 kA. Rodger et al. [16] found an efficiency of about 10% of WWLLN for the intracloud flash with a peak current greater than 50 kA in New Zealand. WWLLN is powerful for the intensive lightning. The location error is about 10 km and the time accuracy is about 30 ms.

In addition, positions and intensity of typhoons at 3–6-hourly intervals are obtained from National Meteorological Center of Chinese Meteorology Administration (CMA). There were 94 tropical cyclones and 56 of them were strengthened into typhoons or super typhoons during 2005 to 2008. We choose seven super typhoons that made landfall in China, including Haitang, Talim, Chanchu, Saomai, Sepat, Jangmi, and Sinlaku. Figure 1 shows their pathways. All of these typhoons caused significant economic lost and human casualties. For example, Saomai brought heavy rain and wind to the east coast of China. It was responsible for 483 deaths, 138 missing, and $19.66 billion in damage. The CMA reported that Saomai was the strongest typhoon that ever occurred in China's offshore region as well as the most powerful typhoon ever to make landfall over Mainland China (http://www.typhoon.gov.cn).

Although the typhoons were moving, the maximum speed was only 25 km h^{-1} for the studied typhoons. Given that the occurrence of lightning flash is transient and not very frequent, it is reasonable to use the flashes occurring within one hour in 800 km of the typhoon center to represent the lightning activity at the time of typhoon location. Only six-hourly locations are provided at the tropical de-

1) Solorzano N N, Thomas J N, Holzworth R H, et al. Global studies of tropical cyclones using the World Wide Lightning Location Network. In: The AMS Annual Meeting 2008 in New Orleans (January 2008).

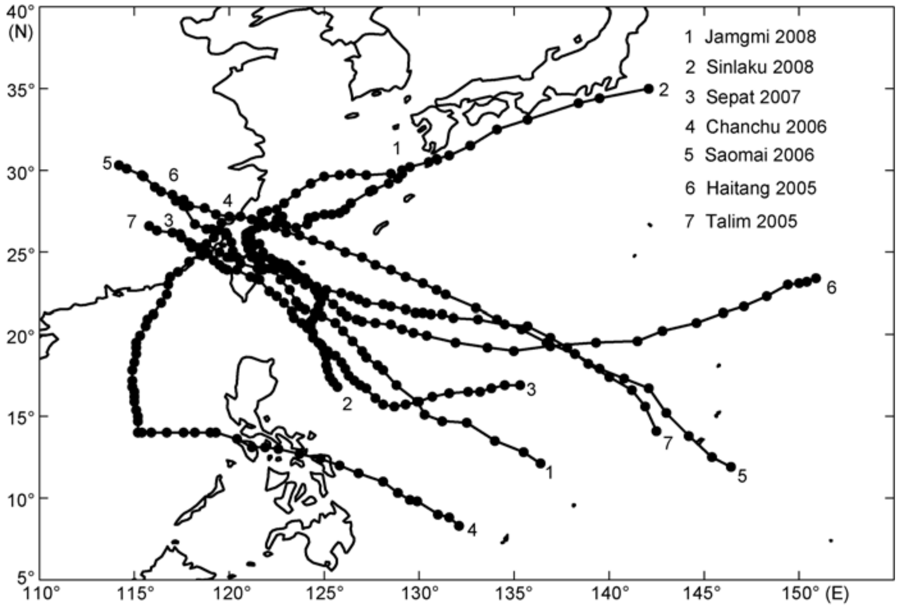

Figure 1 Paths of the 7 super typhoons from 2005 to 2008 analyzed in this study.

pression stage, so the hourly center positions are obtained by the method of spline interpolation. Generally, the diameter of typhoon is 600 to 1000 km, but sometimes it can reach 2000 km and the smallest is only 100 km [18]. In this paper, the diameter of typhoon was chosen as 1600 km based on the MTSAT-1R images (http://agora.ex.nii.ac.jp/digital-typhoon) of the seven typhoons.

2 The overall characteristics of lightning activity in the seven typhoons

Table 1 lists the statistic characteristics of seven super typhoons that landed China during 2005–2008. It can be seen that, despite a large variance in lightning number owing to the size difference of individual typhoons, an average number of 2000–3000 flashes per day occurred within 800 km of the typhoon center; the maximum was up to 7496 in Sepat typhoon and the minimum only 613 in Saomai. Given that the CG detection efficiency is only 26% and the total lightning is less than 13% [15, 16], the lightning activity in typhoon is still active, although the flash frequency is lower than that in MCS and hail storms, whose representing values were about 260 fl (5 min)$^{-1}$ [19] and 55 fl min^{-1} [20], respectively.

For the seven typhoons, less than 1% of the flashes occurred within 100 km of the center. In contrast, Molinari et al. [7] found that less than 1% lightning occurred within 40 km and 4.3% within 80 km. The difference may be due to the different typhoon scale in the Pacific and Atlantic. After a typhoon made its landfall, lightning sharply decreased in the typhoon center possibly because that the typhoon lost water vapor supplied by the ocean and surface friction leading to the eye disappeared. However, the flashes in the center of Saomai typhoon were still active after its landfall. Saomai was the most intense landfall typhoon since the 1950s in mainland China, in which eye was still clear and the maximum sustained wind was as high as 60 m s^{-1} after its landfall.

2.1 Radial distribution of lightning activity

There are three distinct zones in radial direction of typhoon, eye, eyewall, and rainbands, and the rainbands can be further divided into inner rainbands and outer rainbands. Inner rainbands vary in location from storm to storm but typically lie between 50 and 100 km from the eye wall. The cloud in inner bands is generally stratiform. Unlike the eyewall, the convection in inner bands is much weaker. Inner bands are connected between eyewall and outer bands [21].

The mature stage of typhoon in this paper means when the maximum sustained wind reached at 32.7 m s^{-1}. Lightning density used in this paper is referred to an area of 100 km×100 km. Lightning flashes are divided into 20 km annular rings beginning from the storm center and continuing outward to 800 km, and most or all flashes associated with typhoon should be counted in this way. The typhoons are divided into two groups based on the flash density, one with maximum flash density exceeding 200 fl (100 km)$^{-2}$ day^{-1}, and the other less than 120 fl (100 km)$^{-2}$ day^{-1}.

Figure 2(a) and (b) show the distribution of flash density in the radial direction. The radial distributions generally showed three common regions in the seven typhoons. The first region was a lightning maximum in 20–80 km of ty-

Table 1 List of seven typhoons and their lightning activities

Name	Pressure (hPa)	Wind (m s^{-1})	Begin and end	Time (h)	800 km average flashes (fl day^{-1})	Flash number					
						TD–STS[a)]		Whole life		After landfall	
						<100 km	<800 km	<100 km	<800 km	<100 km	<800 km
Jangmi (0815)	910	65	09-24 20:00 10-01 02:00	151	2100	33	1687	180	13210	4	2165
Sinlaku (0813)	935	52	09-09 05:00 09-20 08:00	268	3467	1	1772	271	38837	1	595
Sepat (0709)	910	65	08-13 02:00 08-20 02:00	169	7496	637	2437	3912	52776	25	12432
Chanchu (0601)	945	45	05-09 08:00 05-18 08:00	226	3370	112	12864	215	31683	0	676
Saomai (0608)	915	60	08-05 20:00 08-12 05:00	154	613	113	1159	433	3934	71	1220
Haitang (0505)	910	65	07-12 08:00 07-20 17:00	202	2048	141	1078	289	17227	1	6068
Talim (0513)	910	65	08-27 08:00 09-02 07:00	144	2287	1167	9494	1921	13724	0	511

a) TD, Tropical Depression; STS: Severe Tropical Storm.

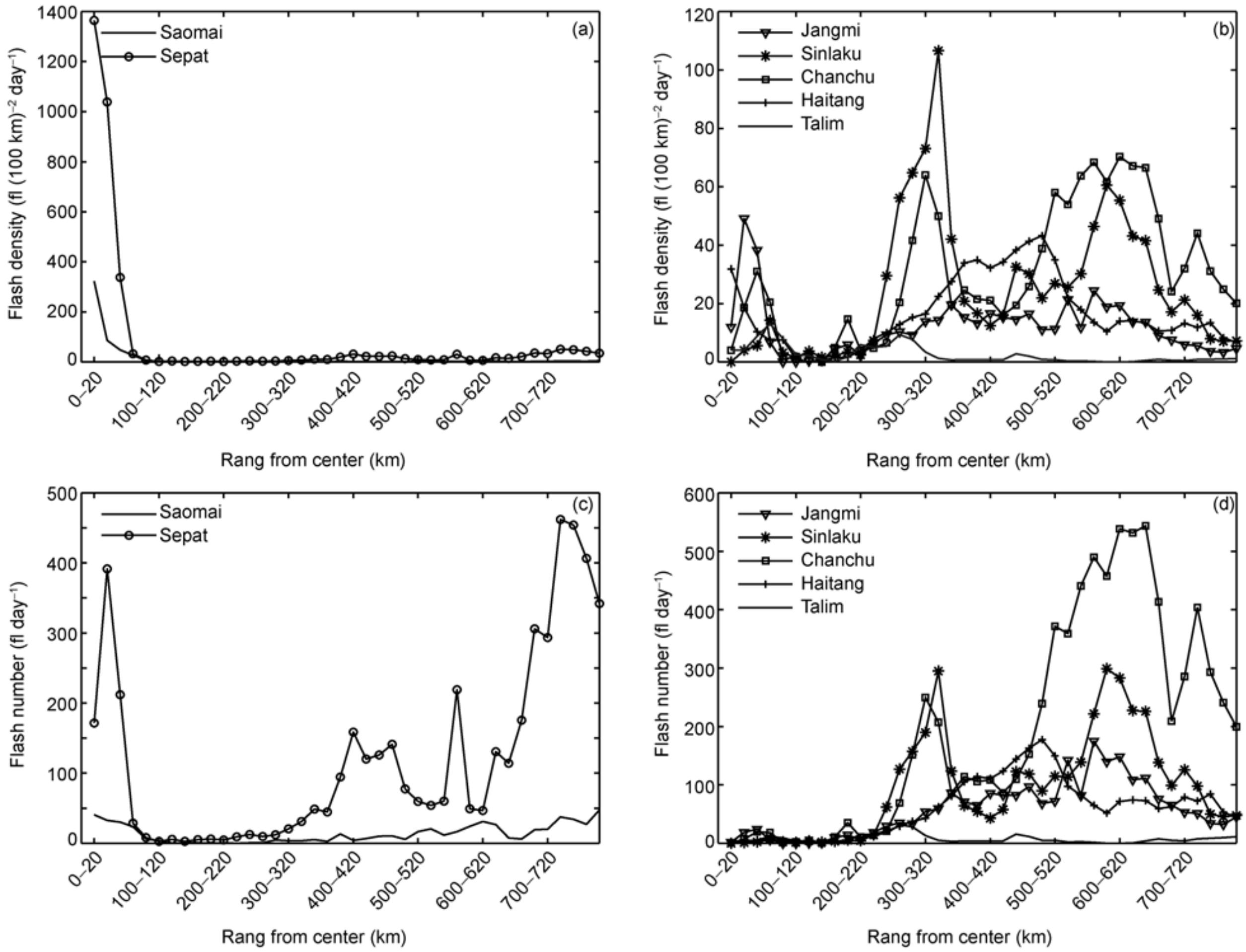

Figure 2 Radial distribution of flash density (unit: fl (100 km)$^{-2}$ day^{-1}). (a) Two typhoons with maximum flash density greater than 200 fl (100 km)$^{-2}$ day^{-1}; (b) five typhoons with maximum flash density less than 120 fl (100 km)$^{-2}$ day^{-1}; and (c) and (d) corresponding radial distribution of flash number (fl day^{-1}).

phoon center, which corresponded to the eyewall region. Flash density in eyewall region of typhoon Sepat, Saomai, and Haitang reached their maximum value in 20 km, and typhoon Jangmi, Sinlaku, Chanchu, and Talim at 40, 80, 60, and 80 km respectively. Sepat's maximum flash density in eyewall exceeded 1346 fl (100 km)$^{-2}$ day^{-1}, whereas Saomai's was also higher than 300 fl (100 km)$^{-2}$ day^{-1}. The other five typhoons had an eyewall maximum between 13 to

50 fl (100 km)$^{-2}$ day^{-1}. The second region was a lightning minimum in 100–200 km of the center. The last one was outer rainbands, another lightning maximum outside 200 km. The lightning flash density in outer rainbands was less than 5 fl (100 km)$^{-2}$ day^{-1} in Saomai, and no more than 50 (100 km)$^{-2}$ day^{-1} in Sepat's. Two peak values appeared in Sinlaku and Chanchu, one at about 300 km, and the other at about 600 km. There was only one peak in Jangmi, Haitang, and Talim.

Figure 2(c) and (d) shows the radial distribution of the flash number. Both of the flash number and density in Sepat typhoon were the maximum, whereas those in others were much lower. The radial distribution of flash number was similar to that of flash density.

2.2 Spatial distribution of lightning activity

Figure 3(a) shows composite spatial distribution of lightning activities in the mature stage of the seven typhoons normalized to each center. The three lightning regions, inner core and outer rainbands flash maximum, and the intermediate flash minimum, show clearly. An asymmetric distribution of lightning was quite distinct, most of them occurred in Southeast quadrant, and a few were located in the right of the motion path. Lightning tended to occur in deep convective cloud, and clustered in outer spiral rainbands. Figure 3(b) shows spatial distribution of lightning in Haitang at its intensity peak day. A few lightning flashes occurred in the core, and the eye could not be distinguished. Lightning in 60–300 km of the center was near zero and a 200 km wide lightning band were found in outer bands.

Because the typhoon moved slowly, no significant change could be found in the cloud image. So five-hours lightning flashes are overlaid on the same visible cloud image. The eye of Jangmi can be clearly seen from Figure 3(c), which was relatively smaller. A 30 km wide lightning band surrounded the eye. The lightning frequency in Chanchu was much higher than that of Jangmi. The eye of Chanchu was also clear, and its radius was about 50 km, much larger than that in Jangmi. A 30 km ring band of lightning was

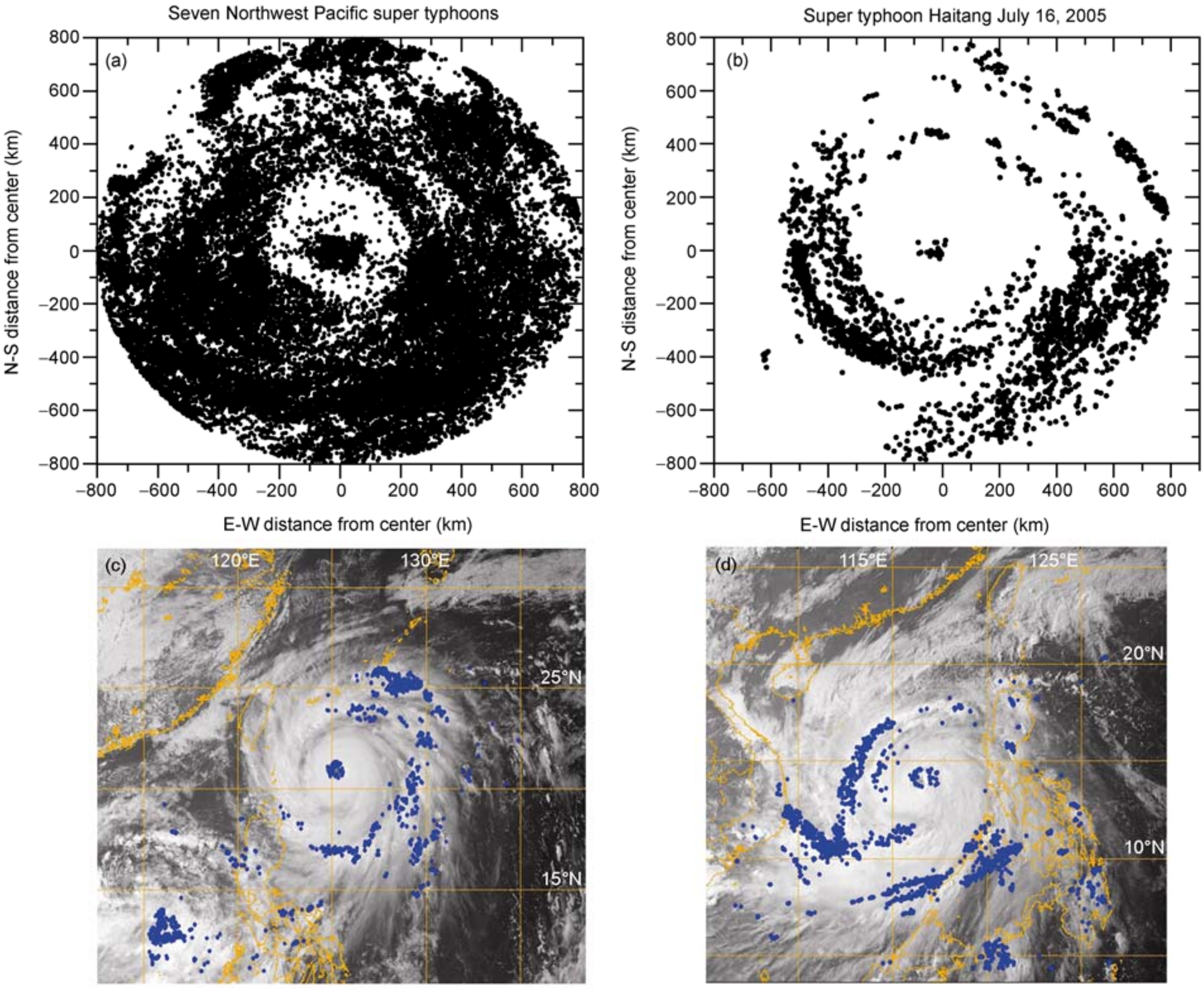

Figure 3 (a) Normalized lightning distribution in 7 typhoons; (b) lightning distribution in mature stage of Haitang; (c) and (d) lightning (blue dots) distribution in mature stage of Jangmi and Chanchu superimposed on the corresponding satellite images.

embodied in eyewall, a few flashes occurred in inner rainbands and lightning increased in outer rainbands. This radial distribution is consistent with the convective structure of a mature typhoon. We define the lightning within 100 km of the center as eyewall lightning or center lightning, and lightning within 800 km as average lightning base on the study above.

2.3 The lightning evolution in time

Little is known about the lightning evolution during the whole lifetime of typhoon so far, mainly because of the limitation of the observation means. Figure 4(a) shows the evolution of lightning frequency within 800 km for Jangmi, along with 6- and 3-h maximum sustained wind (similar tendency for other six typhoons, but not shown). Peaks in lightning activity were observed several hours before the typhoon reached its peak intensity, and the largest peak occurred during the landfall period of typhoon.

According to the integrated satellite images and MTSAT-1R satellite images from the Naval Research Laboratory (NRL) and the Japan Digital Typhoon Network to determine the typhoon eye appearance time. Figure 4(b)–(h) shows the information on evolution of lightning activities within 100 km of the center, time of eye appearing, eyewall replacement, and typhoon landfall, and so on.

Figure 4(b) shows the eyewall lightning of Haitang in histogram, along with the maximum sustained wind and minimum pressure. The eye appeared at 05:00, July 15. A lightning outbreak occurred during the fast enhancement stage of typhoon and prior to the time when wind reached its maximum. No lightning occurred during the periods of its most intensive stage of typhoon Haitang (12:00 July 16–00:00 July 17). From the 85 GHz TMI of TRMM (not shown), double eyewalls can be identified clearly. After the eyewall replacement, there was no lightning in typhoon center.

A lightning outbreak occurred in typhoon Talim six hours before the maximum intensity (refer to Figure 4(c)). The lightning in Talim was less than that in Haitang. During the TD-STS stage, lightning activity in Talim was the most active, comparing with other typhoons. However, after the eyewall replacement, no lightning happened in the center. Figure 4(d) shows lightning evolution of typhoon Chanchu, which struck the Philippines twice as a typhoon during May 12–13, upgraded to a super typhoon while in the South China Sea, and hit Guangdong Province. Lightning outbreak occurred one day before it reached its maximum intensity. Sepat and Jangmi also showed their lightning outbreak several hours prior to or at their maximum intensity, and a few flashes occurred during the periods of weakening. Very few flashes activities were found in Sinlaku through its whole lifetime. On the mean, the eyewall lightning outbreak during the periods of its intensification, usually several hours prior to its maximum intensity, but some individual outbreaks during the maximum stage. During the maximum stage of typhoon, the outer eyewall started to replace the inner eyewall in some intense storms [22]. A few average flashes occurred during the maximum stage. Since the eyewall replacement, flashes happened in eyewall region was nearly zero.

3 Summary and discussions

Data from the WWLLN have been used to investigate the lightning activities in seven typhoons over Northwest Pacific ocean. Though the efficiency of WWLLN is much lower than NLDN, it can basically reflect lightning activities and provide continuous and high quality lightning locations in typhoon. Some results are summarized below.

(1) Although the spatial distribution of lightning in each typhoon was not exactly the same, basically three distinct average flash density regions in mature typhoon were found, eyewall and outer rainbands were two regions with active lightning, and inner bands with near-zero lightning. The eyewall shows almost the highest cloud top in the typhoon. There are only updrafts and no downdrafts in the eyewall, leading to a few flashes occurred in this region, compared with terrestrial convective clouds [18]. Jorgensen [2], Marks [23], and Black et al. [24] found that typical updraft velocities in the eyewall was less than 8 m s^{-1}. More extreme updrafts occasionally were found, but in general hurricanes updrafts were much weaker than continental updrafts. Hurricane rainbands were found to have slightly weaker updraft magnitudes than eyewalls. Typical values for mean vertical velocities in eyewall updrafts are ~4 m s^{-1}, with maximum vertical velocities typically of 7–8 m s^{-1}. Interestingly, a few flashes occurred in eyewall in the latter of the maximum intensity stage, though the cloud top was still high.

(2) Flash in outer rainbands was quite asymmetric and appeared as cluster in deep cloud. Lightning flashes in outer rainbands were far more than those in the center. Less than 1% of flashes occurred within 100 km of the center.

(3) Lightning in the center decreased sharply after typhoon landfall and even no lightning occurred in some typhoons. The water vapor supply is reduced and energy source missed as the landfall of typhoon. Furthermore, the factors such as surface friction and inflow of cool air to the low-level center result in rapid weakening of the typhoon, and consequently, lightning activity in the typhoon center decreases.

(4) Eyewall lightning outbreak occurred several hours before or just as its intensity reaching its maximum, indicating that the lightning activities could be used as a proxy to forecast typhoon intensity. On the weakening stage, little or even no lightning occurred in the center of typhoon.

What could be the possible reason for the occurrence of lightning in typhoon? Black and Hallett [25], using recon-

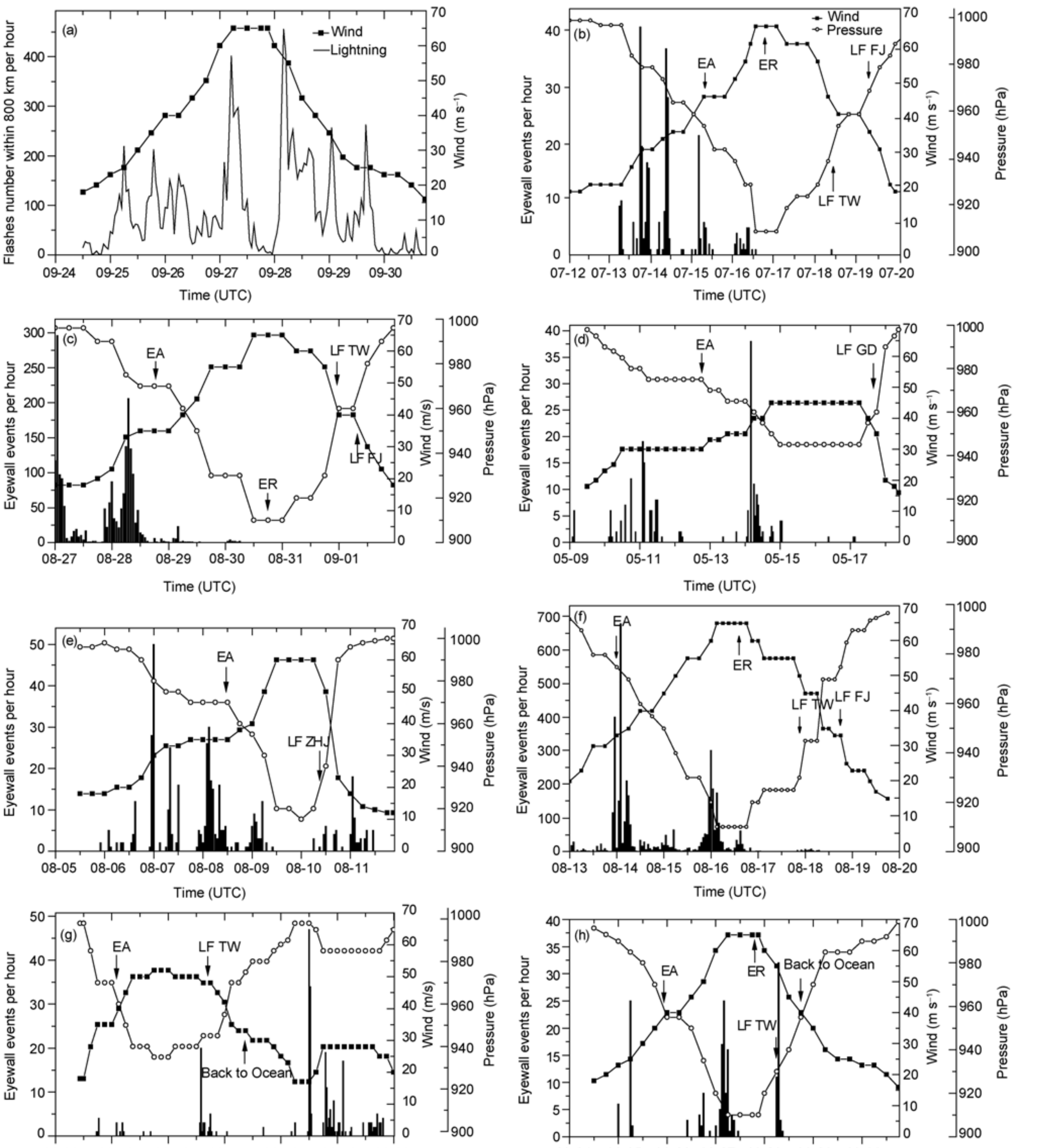

Figure 4 (a) Evolution of hourly lightning activity of Jangmi within 800 km of the typhoon center; (b)–(h) histogram of typhoon eyewall lightning (within 100 km of the typhoon center), along with the maximum sustained wind and the minimum pressure ((b) Haitang, (c) Talim, (d) Chanchu, (e) Saomai, (f) Sepat (g) Sinlaku, (h) Jangmi). TW, Taiwan; ZHJ, Zhejiang; FJ, Fujian; GD, Guangdong; EA, Eye Appearance; ER, Eyewall Replacement; LF, Land Fall.

naissance aircraft data through three Atlantic hurricanes, found the existence of supercooled drops, graupels, columns, and aggregated snowflakes in the hurricanes. The supercooled drops were found only in convection updrafts larger than 5 m s^{-1}. Soon after, they made a summary of the flights records in about 20 years [26], and found that lightning occurrence in a number of storms could be related with strong velocity (>10 m s^{-1}) and the supercooled liquid cloud droplets could extend below –20°C. In the systems with stronger vertical velocity, there is a larger region of supercooled cloud extending to lower temperature where charge separation may occur, as judged by the presence of regions containing graupel, small ice, and cloud droplets.

Only seven super typhoons have been studied in this study, more cases are needed to confirm the results. However, the results of the seven typhoons are consistent to some extent. The spatial and temporal distribution of lightning in other tropical cyclones will be examined extensively. No enough knowledge has been gained about the microphysical processes in typhoon, so it is hard to conclude concisely the relationship between lightning activity and microphysics, and further studies on microphysics and electrification mechanisms are needed. Numerical model coupling with electrification processes will also be utilized to study the mechanisms of lightning in typhoon.

We thank all of the hosts of WWLLN and Washington University who provided lightning dataset. Typhoon data are provided by CMA, and cloud images are provided by NRL. This work was supported by Knowledge Innovation Project of the Chinese Academy of Sciences (Grant No. KZCX2-YW-206) and 100 Talents Program of Chinese Academy of Sciences.

1 Chen L S, Meng Z Y. An overview on tropical cyclone research progress in China during the past ten years (in Chinese). Chin J Atmos Sci, 2001, 25: 420–432
2 Jorgensen D P, Zipser E J, LeMone M A. Vertical motions in intense hurricanes. J Atmos Sci, 1985, 42: 839–856
3 Christian H J, Blakeslee R J, Boccippio D J, et al. Global frequency and distribution of lightning as observed from space by the Optical Transient Detector. J Geophys Res, 2003, 108: 4005
4 Molinari J, Moore P K, Idone V P, et al. Cloud-to-ground lightning in Hurricane Andrew. J Geophys Res, 1994, 99: 16665–16676
5 Samsury C E, Orville R E. Cloud-to-ground lightning in tropical cyclones: A study of Hurricanes Hugo (1989) and Jerry (1989). Mon Weather Rev, 1994, 122: 1887–1896
6 Lyons W A, Keen C S. Observations of lightning in convective supercells within tropical storms and hurricanes. Mon Weather Rev, 1994, 122: 1897–1916
7 Molinari J, Moore P, Idone V. Convective structure of hurricanes as revealed by lightning locations. Mon Weather Rev, 1999, 127: 520–534
8 Cecil D J, Zipser E J. Relationships between tropical cyclone intensity and satellite-based indicators of inner core convection: 85-GHz ice-scattering signature and lightning. Mon Weather Rev, 1999, 127: 103–123
9 Cecil D J, Zipser E J, Nesbitt S W. Reflectivity, ice scattering, and lightning characteristics of hurricane eyewalls and rainbands. Part I: Quantitative description. Mon Weather Rev, 2002, 130: 769–784
10 Cecil D J, Zipser E J. Reflectivity, ice scattering, and lightning characteristics of hurricane eyewalls and rainbands. Part II: Intercomparison of observations. Mon Weather Rev, 2002, 130: 785–801
11 Squires K, Businger S. The morphology of eyewall lightning outbreaks in two category 5 hurricanes. Mon Weather Rev, 2008, 136: 1706–1726
12 Shao X M, Harlin J, Stock M, et al. Katrina and Rita were lit up with lightning. EOS, 2005, 86: 398–399
13 Crombie D D. Periodic fading of VLF signals received over long paths during sunrise and sunset. J Res Nat Bur Stand Sect D-Radio Sci, 1964, 68: 27–34
14 Lay E H, Holzworth R H, Rodger C J, et al. WWLL global lightning detection system: Regional validation study in Brazil. Geophys Res Lett, 2004, 31: L03102
15 Rodger C J, Brundell J B, Dowden R L. Location accuracy of VLF World Wide Lightning Location (WWLL) network: Post-algorithm upgrade. Ann Geophys, 2005, 23: 277–290
16 Rodger C J, Werner S, Brundell J B, et al. Detection efficiency of the VLF World-Wide Lightning Location Network (WWLLN): Initial case study. Ann Geophys, 2006, 24: 3197–3214
17 Jacobson A R, Holzworth R H, Harlin J, et al. Performance assessment of the World Wide Lightning Location Network (WWLLN), using the Los Alamos Sferic Array (LASA) array as ground-truth. J Atmos Ocean Technol, 2006, 23: 1082–1092
18 Zhu Q G, Lin J R, Shou S W, et al. Principles and Methods of Synoptic Meteorology (in Chinese). 3rd ed. Beijing: China Meteorological Press, 2000. 509–516
19 Liu D X, Qie X S, Feng G L, et al. Analyses on lightning temporal and spatial characteristics in the severe convective weather in North China (in Chinese). Plateau Meteorol, 2008, 27: 358–364
20 Feng G L, Qie X S, Yuan T, et al. Lightning activity and precipitation structure of hailstorms. Sci China Ser D-Earth Sci, 2007, 50: 629–639
21 Chen L S, Dind Y H. Overview of the Western Pacific Typhoon (in Chinese). Beijing: Science Press, 1979. 59–60
22 Houze R A, Chen S S, Smull W C, et al. Hurricane intensity and eyewall replacement. Science, 2007, 315: 1235–1239
23 Marks F D Jr. Evolution of the structure of precipitation in Hurricane Allen (1980). Mon Weather Rev, 1985, 113: 909–930
24 Black M L, Burpee R W, Marks F D Jr. Vertical motion characteristics of tropical cyclones determined with airborne Doppler radial velocities. J Atmos Sci, 1996, 53: 1887–1909
25 Black R A, Hallett J. Observations of the distribution of ice in hurricanes. J Atmos Sci, 1986, 43: 802–822
26 Black R A, Hallett J. Electrification of the Hurricane. J Atmos Sci, 1999, 56: 2004–2028